ARTICLE

A 3D atlas of the human developing pancreas to explore progenitor proliferation and differentiation

Adrian Villalba[1] · Yorick Gitton[2] · Megumi Inoue[2] · Virginie Aiello[1] · Raphaël Blain[2] · Maryne Toupin[3] ·
Séverine Mazaud-Guittot[3] · Latif Rachdi[1] · Henrik Semb[4] · Alain Chédotal[2,5,6] · Raphaël Scharfmann[1]

Abstract

Aims/hypothesis Rodent pancreas development has been described in great detail. On the other hand, there are still gaps in our understanding of the developmental trajectories of pancreatic cells during human ontogenesis. Here, our aim was to map the spatial and chronological dynamics of human pancreatic cell differentiation and proliferation by using 3D imaging of cleared human embryonic and fetal pancreases.

Methods We combined tissue clearing with light-sheet fluorescence imaging in human embryonic and fetal pancreases during the first trimester of pregnancy. In addition, we validated an explant culture system enabling in vitro proliferation of pancreatic progenitors to determine the mitogenic effect of candidate molecules.

Results We detected the first insulin-positive cells as early as five post-conceptional weeks, two weeks earlier than previously observed. We observed few insulin-positive clusters at five post-conceptional weeks (mean ± SD 9.25±5.65) with a sharp increase to 11 post-conceptional weeks (4307±152.34). We identified a central niche as the location of onset of the earliest insulin cell production and detected extra-pancreatic loci within the adjacent developing gut. Conversely, proliferating pancreatic progenitors were located in the periphery of the epithelium, suggesting the existence of two separated pancreatic niches for differentiation and proliferation. Additionally, we observed that the proliferation ratio of progenitors ranged between 20% and 30%, while for insulin-positive cells it was 1%. We next unveiled a mitogenic effect of the platelet-derived growth factor AA isoform (PDGFAA) in progenitors acting through the pancreatic mesenchyme by increasing threefold the number of proliferating progenitors.

Conclusions/interpretation This work presents a first 3D atlas of the human developing pancreas, charting both endocrine and proliferating cells across early development.

Keywords Human fetal pancreas · Insulin-producing cells · Light-sheet fluorescence microscopy · Pancreatic progenitors · PDGF signalling · Proliferating cells · Type 1 diabetes

---

Adrian Villalba and Yorick Gitton contributed equally.

✉ Alain Chédotal
alain.chedotal@inserm.fr

✉ Raphaël Scharfmann
raphael.scharfmann@inserm.fr

1 Institut Cochin, CNRS, Inserm, Université Paris Cité, Paris, France

2 Inserm, CNRS, Institut de la Vision, Sorbonne Université, Paris, France

3 Inserm, EHESP, IRSET (Institut de Recherche en Santé, Environnement et Travail), UMR_S 1085, Université Rennes, Rennes, France

4 Institute of Translational Stem Cell Research, Helmholtz Diabetes Center, Helmholtz Zentrum München, München, Germany

5 Institut de pathologie, groupe hospitalier Est, hospices civils de Lyon, Lyon, France

6 MeLiS, CNRS UMR5284, Inserm U1314, University Claude Bernard Lyon 1, Lyon, France

Research in context

What is already known about this subject?

- Rodent pancreas development is well documented, but the underlying mechanisms for human pancreas formation and maturation are less understood

- Previous single-cell RNA-seq studies on the developing human pancreas lack the assessment of topographic relationships between pancreatic progenitors and endocrine cell types

- Recently, the combination of light-sheet fluorescence microscopy with tissue clearing allowed 3D visualisation of cellular and tissue architecture, which had not previously been performed for the human fetal pancreas

What is the key question?

- What are the spatial locations of the earliest insulin-positive cells and proliferating pancreatic progenitors across human pancreatic development during the first trimester of pregnancy?

What are the new findings?

- The earliest insulin-positive cells appear at around post-conception week 5 and are located in the inner part of the pancreas, suggesting the existence of a niche for differentiation

- Embryonic and fetal human pancreatic proliferating progenitors are restricted to the periphery of the developing pancreas

- The AA isoform of platelet-derived growth factor (PDGFAA) induces the proliferation of pancreatic progenitors in vitro

How might this impact on clinical practice in the foreseeable future?

- This knowledge may offer substantial contributions towards the improvement of protocols to generate stem cell-derived beta cells for therapeutic purposes in type 1 diabetes

Abbreviations

ALK5i	ALK5 inhibitor
CPA1	Carboxypeptidase A1
ECAD	Epithelial cadherin
FGF	Fibroblast growth factor
HuDeCA	Human Developmental Cell Atlas
INS	Insulin
LSFM	Light-sheet fluorescence microscopy
NKX6.1	NKX homeobox 1
PCW	Post-conceptional week(s)
PDGF	Platelet-derived growth factor
PDGFAA	PDGF AA isoform
PDGFRA	PDGF receptor α
PDGFRB	PDGF receptor β
PDX1	Pancreatic and duodenal homeobox 1
RT	Room temperature
SOX9	SRY-box transcription factor 9
SUSD2	Sushi domain containing 2

Introduction

The pancreas is a vital organ involved in multiple crucial functions from glucose homeostasis to digestion [1]. It is a mixed gland composed of an exocrine and an endocrine fraction. The exocrine part contains acinar cells releasing enzymes like carboxypeptidase A1 (CPA1) and amylase through a ductal network draining into the duodenum. The endocrine fraction, clustered in the islets of Langerhans, accounts for 1% of the pancreatic mass. Pancreas dysfunction is associated with a large spectrum of disorders, including diabetes mellitus, pancreatitis and pancreatic cancer, which are major health burdens worldwide [2]. During embryonic development, the pancreas originates from the foregut endoderm and undergoes morphogenesis, characterised by extensive proliferation, migration and differentiation of distinct cell populations [3]. Among them, the endocrine cells, which produce hormones such as insulin (INS; beta cells), glucagon (alpha cells), and somatostatin (delta cells), are derived from a subset of pancreatic progenitor cells that undergo endocrine differentiation [1]. Understanding the

regulation of this process is the subject of intense research, bearing significant implications for developmental biology and regenerative medicine [4, 5].

Rodent pancreas development has been studied in great detail during the past decades [6]. However, the developmental and cellular mechanisms underlying the formation and maturation of the human pancreas are far less understood. The development of the human pancreas begins during the fourth post-conceptional week (PCW), when dorsal and ventral pancreatic buds emerge from the endodermal cells of the developing gut tube [7]. These epithelial buds contain pancreatic progenitors that express key transcription factors such as pancreatic and duodenal homeobox 1 (PDX1), SRY-box transcription factor 9 (SOX9), NKX homeobox 1 (NKX6.1), forkhead box A2 (FOXA2) and pancreas-associated transcription factor A (PTF1A) [8]. They develop in an intricate fashion within the surrounding mesodermal-derived mesenchyme and undergo fusion, branching morphogenesis, differentiation of endocrine and exocrine cells, and establishment of functional connections with the surrounding organs [7]. Pancreatic progenitor cell differentiation into endocrine cells is tightly regulated by various transcription factors and signalling pathways [9]. In this context, the way the human pancreas develops represents a critical source of information [7].

Recently, the combination of light-sheet fluorescence microscopy (LSFM) and tissue clearing has enabled the three-dimensional (3D) visualisation of cellular and tissue architecture in unprecedented detail and resolution [10, 11]. Moreover, the integration of imaging data across different developmental stages has led to the creation of tissue atlases, providing comprehensive cellular maps [12].

So far, 2D descriptions have not captured the topographic relationship between pancreatic progenitors and endocrine cell types. In this study, we leveraged our expertise in LSFM and tissue clearing [13] to revisit the early stages of human pancreas development (PCW5–11), which retain their topographic integrity. We specifically aimed at investigating the spatiotemporal dynamics of INS$^+$ cell differentiation and progenitor proliferation in the developing human pancreas using LSFM to build a human developing pancreas atlas. Our results reveal novel insights into the cellular mechanisms underlying pancreatic development and provide a foundation for future studies aimed at gaining further insights into human pancreas development.

Methods

Human and mouse embryonic and fetal pancreatic tissues Human embryonic and fetal pancreatic tissues (PCW5–11) were obtained through the Inserm cross-cutting scientific programme Human Developmental Cell Atlas (HuDeCA)

from surgical abortions in accordance with the French bioethics legislation and Inserm guidelines [14, 15]. Donors' written consent was obtained, along with approval from Agence de Biomédecine, the competent authority in France. Fetal ages are displayed as PCW, staged based on morphometric correction [16]. All specimens were initially selected based on macroscopic morphological criteria, excluding samples with obvious malformations. In cases where visual determination of sex was not possible, PCR-based chromosome screening using DNA from biopsies was performed [13]. For labelling, a minimum of three samples per age were employed (electronic supplementary material [ESM] Table 1 and ESM Table 2), while for in vitro experiments we employed a minimum of five pancreases per condition.

Mouse fetal pancreases were obtained from pregnant C57BL/6J mice purchased from the Janvier Breeding Center (LeGenet, St Isle, France). Mice were killed by CO_2 asphyxiation according to French Animal Care Committee guidelines and pancreases from embryos at embryonic day (E)10, E12 and E16 (at least six embryos per age) were dissected and fixed [17].

Conventional 2D immunohistochemistry Human embryonic and fetal pancreases were fixed in formalin, embedded in paraffin and sectioned (5 μm thick) as previously described [14]. The primary and secondary antibodies used are listed in ESM Table 3. EdU revelation was performed using the Click EdU Alexa 555 imaging kit (Thermo Fisher Scientific, Waltham, MA, USA). Nuclei were stained with Hoechst 33342 (0.3 mg/ml, Invitrogen, Waltham, MA, USA).

We manually counted the number of INS$^+$ cells per cluster in all the 5 μm sections of three pancreases at PCW6 (180–240 sections/specimen). The percentage of PDX1$^+$/ KI67$^+$ (at PCW7, 9 and 11) and INS$^+$/KI67$^+$ cells (at PCW9 and 11) were quantified on six sections per pancreas (3 pancreases/age). The spatial distribution of PDX1$^+$/KI67$^+$ progenitors was measured by computing the Ripley K function [$K(r)$] [18]. To do that, the PDX1$^+$/KI67$^+$ progenitors were mapped with x,y coordinates in 2D images at PCW7, 9 and 11 (minimum of n=20 images/developmental stage), using FIJI (version 2.14.0, Eliceirei/LOCI group, USA) [19]. Then, $K(r)$ was computed for every image by implementing the R (version 4.1.2, R Foundation for Statistical Computing, Austria) library spatstat as previously described [20].

3D immunostaining Embryonic and fetal samples were fixed by immersion in formalin at 4°C for 1 to 5 days depending on size. For tissue bleaching [10], fixed pancreases were dehydrated for 1 h at room temperature (RT) in increasing concentrations of methanol (50%, 80%, 100%) in 1X PBS. Then, the samples were incubated overnight at 4°C in a 6% hydrogen peroxide solution in 100% methanol, re-hydrated for 1hr at RT in decreasing concentrations of

methanol (100%, 100%, 80%, 50%) and finally washed for 1 h in 1X PBS. Permeabilisation and blocking were performed under rotation at 70 rev/min at RT in PBSGT (1X PBS, 0.2% gelatin [Prolabo, Nemours, France], and 0.5% Triton X-100 [Sigma-Aldrich, Saint-Louis, MO, USA]) [13].

For whole-mount immunostaining, samples were incubated with the primary antibodies in a solution of PBSGT containing 0.1% saponin during 14 days at 37°C under rotation at 70 rev/min. The primary and secondary antibodies employed are listed in ESM Table 3. Then, tissues were incubated with the secondary antibodies in a solution of PBSGT (0.1% saponin [10 mg/ml]), during 4 days at 37°C under rotation at 70 rev/min. Next, samples were washed for 30 min in PBSGT at RT, embedded in 1.5% agarose (Roth, Goshen, IN, USA) prepared in TAE 1X (Invitrogen) [10, 11] and stored at 4°C until tissue clearing.

In order to achieve tissue transparency, the samples were cleared using a modification from the iDISCO+ protocol [21]. Fetal pancreases were dehydrated in growing concentrations of methanol (20%, 40%, 60%, 80%, 100%, 100%, 1 h each) at RT under rotation (14 rev/min), next incubated overnight in a solution of 2/3 dichloromethane (DCM) and 1/3 methanol, then for 30 min in 100% DCM, and finally transferred to dibenzyl ether (DBE) for further storage and imaging.

3D imaging and processing Acquisition was performed with Miltenyi Biotec (Bergisch Gladbach, Germany) Ultramicroscope Blaze (sCMOS camera 5.5 MP) and Imspector Pro (version 7.3.2, LaVision Biotec, Germany) acquisition software. Laser light sheets are generated at excitation wavelengths of 488, 561, 640 and 785 nm. Lenses with 4× magnification (MI Plan 4× NA0.35) and 12× magnification (MI Plan NA0.53) objective were used. The z-step size is 3 μm. Images were generated as tiff files, converted to (.ims) by Imaris File Converter (version 9.8, Bitplane, UK), and the 3D images were reconstructed using the volume rendering function. To isolate a specific region of the tissue, the surface tool was used to manually segment. The 3D images, virtual slices and movies were generated using the snapshot and animation tools. To locate the pancreas in full intact PCW7 human embryo, the SOX9$^+$ pancreatic area was delimited in consecutive slices.

Human and mouse pancreatic lengths and diameters were measured with the distance tool in virtual slices. The measurements of the SOX9$^+$ and INS$^+$ cluster volume and density were performed following the automatic segmentation tool. The distribution of human INS$^+$ clusters was measured in three virtual slices from three different pancreases. First, the pancreatic epithelium was manually outlined and the centroid was determined for each slice. Then, the distance from every INS$^+$ cluster was measured to the centroid [19].

Tissue culture Whole human embryonic and fetal pancreases at PCW6–10 were cultured for a maximum of 7 days at an air-complete medium interface in Petri dishes on 0.45 μm filters (Millipore) [22]. Explants were cultured in G10 medium consisting of RPMI 1640 + glutaMax, 10% FBS, 1% penicillin/streptomycin, 1% HEPES and 1% non-essential amino-acids (61870036, ThermoFisher Scientific). Medium was replaced every 2 days. For EdU incorporation assays, pancreases were treated with 5 μmol/l EdU for 4 h, the reaction was stopped by washing out the tissue with G10 medium and immediate fixation. For experiments with the platelet-derived growth factor (PDGF) AA isoform (PDGFAA), explants were cultured in DMEM/F12 medium (31331, ThermoFisher Scientific) containing ALK5 inhibitor (ALK5i; 10 mmol/l, 221234, Chem Cruz, Dallas, TX, USA), noggin (500 mg/ml, 120–10C, Peprotech, Waltham, MA, USA) and nicotinamide (2.5 mol/l, 481907, Sigma). Explants were treated with PDGFAA (200 ng/ml, PHG0035, Sigma) for 7 days, replacing the medium every 2 days.

Results

Human embryonic and fetal pancreases display isometric growth from 5 to 11 PCW Significant progress in conventional 2D immunostaining has provided highly valuable information about human pancreas development [8]. However, there is limited work providing 3D analyses. Here, we report for the first time the use of iDISCO+ [21] tissue clearing and LSFM to track the morphological development of the human embryonic and fetal pancreas. Conventional immunostainings indicated that pancreatic progenitors are immunoreactive for the transcription factors SOX9, PDX1 and NKX6.1 [7]. We performed triple staining that demonstrated similar pancreatic expression patterns for all three markers in both conventional immunostaining (ESM Fig. 1a) and 3D imaging (ESM Fig. 1b and ESM Video 1). Therefore, during this developmental period PCW5–11, these three markers (SOX9, PDX1 and NKX6.1) can be interchangeably used to identify progenitors. SOX9 staining, in an intact transparent PCW7 human embryo, allowed us to precisely visualise the pancreas in the upper left abdomen, highlighted in magenta (Fig. 1a,b and ESM Video 2). We next immuno-labelled PCW5–11 pancreas for SOX9, followed by clearing and LSFM. In the mouse, the pancreas develops from two independent buds that will fuse later on [23]. However, the timing of this process was poorly documented in humans. At PCW5, both ventral and dorsal buds were detected (Fig. 1c, and ESM Video 3), whereas at PCW6 they had fused and formed a single pancreatic primordium (Fig. 1d).
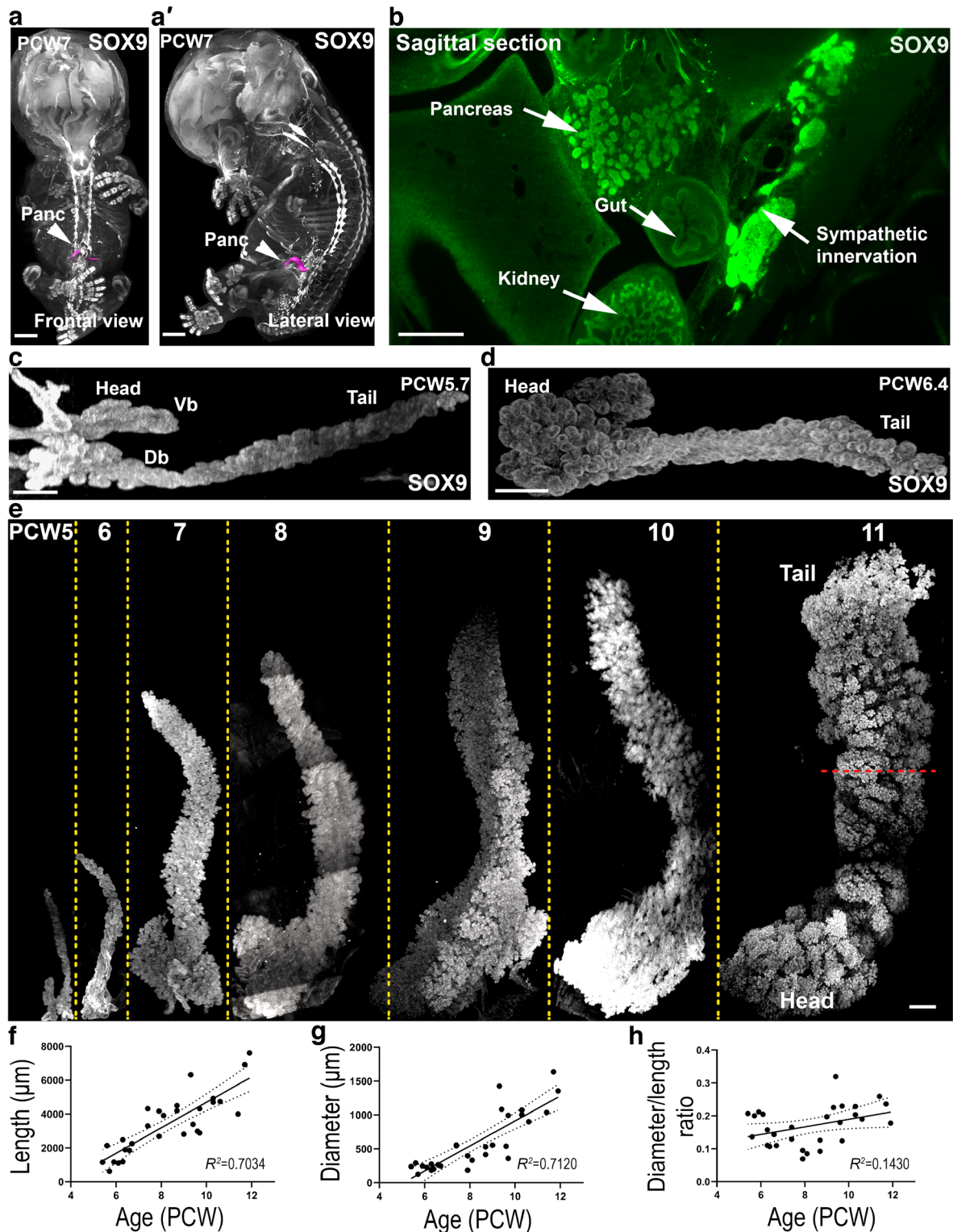
Fig. 1 Human embryonic and fetal pancreases display isometric growth from PCW5 to 11. LSFM images of embryonic and fetal pancreases (**a**–**e**) immunostained for SOX9 or SOX9 and TH (**a**, **a′**, **b**). (**a**, **a′**) Frontal and lateral 3D views of a PCW7 human embryo revealing the anatomical location of the human pancreas (magenta). SOX9 is expressed in the cartilage and various organs including the pancreas. (**b**) Sagittal *z*-stack section of the PCW7 human embryo from Fig. 1a locating the pancreas and adjacent tissues. (**c**, **d**) At PCW5.7, SOX9 staining labels both ventral and dorsal buds, which have fused at PCW6.4. (**e**) Tridimensional SOX9 immunostaining (white) in whole-mount pancreases dissected from human embryos and fetuses between PCW5 and 11. Dashed red line depicts the diameter of the organ. (**f**–**h**) Determination of the length (**f**), the diameter (**g**), and the diameter to length ratio (**h**) of the pancreases from PCW5–11. Scale bars: 2 mm (**a**, **a′**), 500 μm (**b**, **e**), 200 μm (**c**, **d**). Db, dorsal bud; Panc, pancreas; TH, tyrosine hydroxylase; Vb, ventral bud
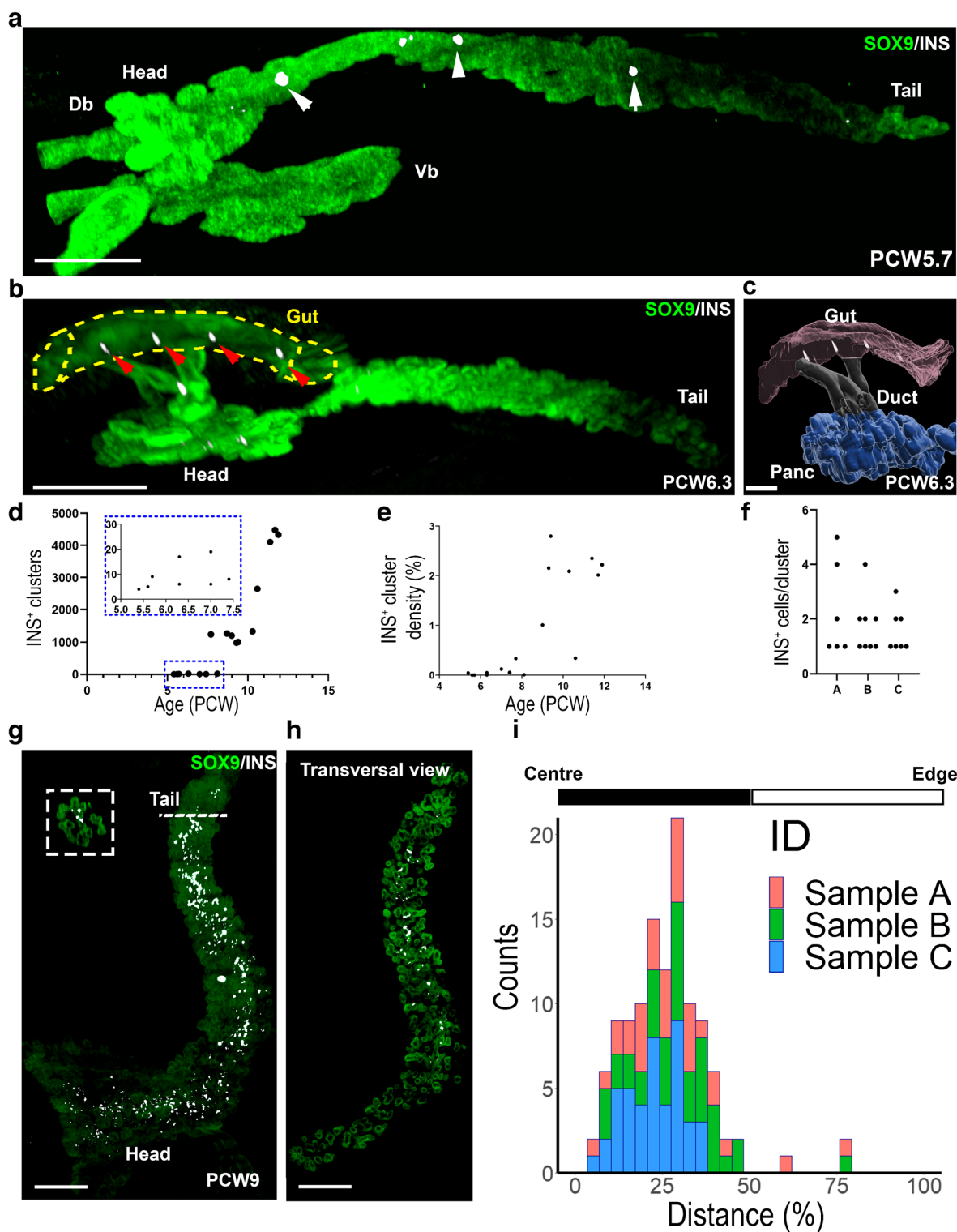
3D imaging in our PCW5–11 series revealed an obvious increase in pancreatic size (Fig. 1e). To quantify human pancreas growth, we measured their lengths along the longitudinal axis and diameters across the dorso-ventral axis. Both length and diameter increased across development from PCW5 to PCW11 (*n*=29 pancreases) (Fig. 1f,g).

The growth in both length and diameter showed a sixfold increase from PCW5 to PCW11, revealing a positive linear correlation between pancreatic size and age. The quantification of the diameter to length ratio showed that it remained stable (Fig. 1h), indicating that pancreas growth is homothetic during the first trimester of gestation.

◀ **Fig. 2** Spatial and time determination of INS$^+$ cell location in the pancreatic primordium. LSFM images of embryonic and fetal pancreases (**a**, **b**, **g**, **h**) immunostained for SOX9 (green) and INS (white). (**a**) At PCW5.7, a few clusters of insulin-immunoreactive (INS$^+$) cells (see white arrows) are found at the centre of the dorsal bud. (**b**) Representative image of extra-pancreatic INS$^+$ cells that were detected in a gut region adjacent to the head of the pancreas (see red arrows) (PCW 6.3) (n=4 pancreases). (**c**) Segmentation of the pancreas, the gut tube and ducts from Fig. 2b, showing the gut region next to the pancreas containing INS$^+$ clusters. (**d**) Determination of the number of INS$^+$ clusters from PCW5–11. (**e**) Determination of INS$^+$ cluster density (volume of INS$^+$ cluster /volume SOX9$^+$ epithelium) from PCW5–11. (**f**) Quantification of the number of INS$^+$ cells per cluster at PCW6, full sectioned and stained to include all the INS$^+$ clusters (n=3) in three different samples (named A, B, and C). (**g**) At PCW9, INS$^+$ clusters are aligned to the centre of the pancreas as shown in 3D. The dashed line represents a sagittal section. (**h**) Transversal view of Fig. 2g. (**i**) Histogram showing the distribution of the INS$^+$ clusters across the pancreatic epithelium in 2D sections from three PCW8 specimens (samples A, B and C). The x-axis represents the distance of the INS$^+$ clusters to the centre of the pancreas. Scale bars: 250 μm (**a**), 300 μm (**b**), 50 μm (**c**), 200μm (**g**, **h**). Db, dorsal bud; Panc, pancreas; Vb, ventral bud

INS$^+$ cells arise around PCW5 and are located in the centre of the human developing pancreas

3D imaging allows the precise spatial location of specific pancreatic cell populations. We next asked when and where the first INS$^+$ cells appear. Previous reports on human fetal pancreases based on 2D immunohistochemistry detected the earliest INS$^+$ cells around PCW7 [8]. Here, we were able to detect the presence of INS$^+$ clusters as early as PCW5.7 (Fig. 2a). At this stage, they were restricted to the dorsal bud and absent from the ventral bud (Fig. 2a, and ESM Video 4), indicating that, as in the mouse [24], INS$^+$ cells first appear in the dorsal pancreas in humans. Recent studies by conventional 2D immunostaining revealed the existence of INS$^+$ cells in the human fetal gut between PCW10 and PCW19 [25]. We could detect extra-pancreatic INS$^+$ clusters far earlier between PCW6.3 and PCW10.6, in the fetal gut next to the pancreas (Fig. 2b,c, and ESM Video 5).

We next quantified the number of pancreatic INS$^+$ clusters on 19 samples between PCW5.4 and PCW11. We observed few INS$^+$ clusters from PCW5.4 to 7.5 (9.25±5.65, mean ± SD, n=8), with a sharp increase at later stages (4307±152.34, mean ± SD, n=3 at PCW11) (Fig. 2d,e). We also manually quantified, using conventional immunostaining, the number of INS$^+$ cells per cluster in paraffin sections from three pancreases (180–240 sections per specimen) at PCW6. We found that the first INS$^+$ clusters contain between 1 and 5 INS$^+$ cells (Fig. 2f).

We next analysed the location of these INS$^+$ clusters and observed their preferential location in the centre of the pancreas, being almost absent from the periphery. INS$^+$ clusters were aligned along the longitudinal axis of the pancreas (Fig. 2g,h and ESM Video 6). We mapped in 3D the distribution of INS$^+$ clusters to the centroid of the SOX9$^+$

pancreatic epithelium in z-slices from 3D scans from three pancreases at PCW9. In all three pancreases, the vast majority of the INS$^+$ clusters were located closer to the centre rather than to the periphery (Fig. 2i).

Our data thus strongly suggest the existence of a niche in the centre of the pancreas promoting the differentiation of progenitors towards an INS$^+$ cell fate. Given that vascularisation has been suggested as an important player in beta cell development in mice [26], we mapped vascular markers with regards to INS$^+$ cells in the human embryonic/fetal pancreas. The general marker for mature vascular endothelial cells CD34 was expressed in a uniform network of vessels intermingled with SOX9$^+$ pancreatic progenitors, without obvious differential distribution from centre to peripheral domains (ESM Fig. 2a). Noticeably, the whole extent of the developing pancreas was devoid of the more specific arterial marker smooth muscle α-actin (SMA) at PCW9 (ESM Fig. 2b).

Finally, we compared pancreatic development between humans and mice by LSFM (ESM Fig. 3a, c). As expected, the number of INS$^+$ clusters increased in mice from E10 to E16 (ESM Fig. 3d and ESM Table 4). Likewise, pancreatic length and diameter increased in mouse embryos between E12 and E16 (ESM Fig. 3e, f). However, the diameter/length ratio increased across development (ESM Fig. 3g), which is different from what we observed in human pancreatic samples from PCW5–11.

Proliferating pancreatic progenitors are restricted to the periphery of the epithelium

Next, we sought to correlate human pancreatic differentiation dynamics with proliferation kinetics across the first trimester. KI67/PDX1 double staining indicated that 20–30% (n=3) of pancreatic progenitors (PDX1$^+$) are in a proliferative state during PCW7–11 (Fig. 3a,b) while differentiated INS$^+$ cells proliferate at a far lower rate at a ratio around 1% at PCW 9–11 (n=3) (Fig. 3c,d).

By selecting cell surface markers and using FACS, we had previously subdivided human fetal pancreatic progenitors into a number of populations with epithelial cadherin (ECAD)$^+$ CD142$^+$ sushi domain containing 2 (SUSD2)$^-$ giving rise to ECAD$^+$CD142$^-$SUSD2$^-$ and finally to ECAD^{low}CD142$^-$SUSD2$^+$ [15]. Here, we first reanalysed our transcriptomic datasets [15], asking whether proliferation markers change from one progenitor population to the other. By using our previously validated list of pancreatic proliferation markers [27], we observed a downregulation from population ECAD$^+$CD142$^+$SUSD2$^-$ to ECAD^{low}CD142$^-$SUSD2$^+$, including canonical proliferation genes such as *KI67* (also known as *MKI67*), *PCNA* and *CDK1* (Fig. 3e). This indicates that progenitors proliferate at different rates in the human embryonic/fetal pancreas and proliferation decreases along with endocrine differentiation.
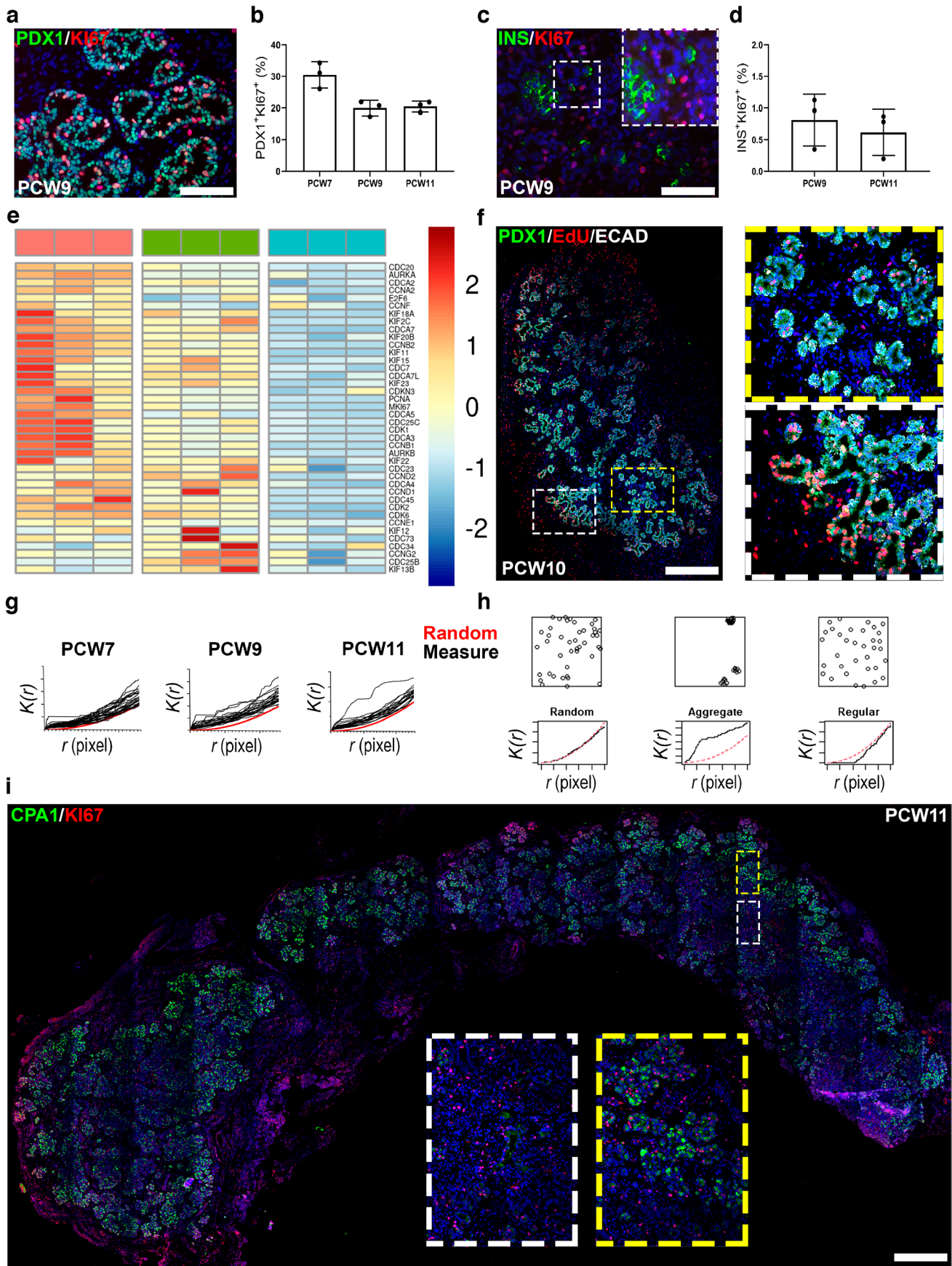
◀**Fig. 3** Proliferation of human embryonic and fetal pancreatic cells. (**a**, **b**) Representative staining for PDX1 (green) and KI67 (red) on sections of human fetal pancreas at PCW9 and quantification of the frequency of PDX1$^+$/Ki67$^+$ at PCW7, 9 and 11 (*n*=3). (**c**, **d**) Representative staining for INS (green) and KI67 (red) on sections of human fetal pancreas at PCW9 and quantification of the frequency of INS$^+$/Ki67$^+$ at PCW9 and 11. Inset reveals a single INS$^+$KI67$^+$ cell. (**e**) Heatmap showing the expression of cell cycle-related genes in three successive populations of pancreatic progenitors: ECAD$^+$CD142$^+$ (pink); ECAD$^+$CD142$^-$ (green); ECAD^{low}CD142$^-$SUSD2$^+$ (blue). The heatmap was generated by the 'heatmap2' function from gplots R package (https://cran.r-proje ct.org/web/packages/gplots/) on standardised log$_2$ expression values from Ramond et al 2018 [15], with Pearson correlation as the distance function. (**f**) Proliferating pancreatic progenitors (PDX1$^+$/ EdU$^+$) across the pancreatic epithelium. PDX1 in green, EdU in red and ECAD in white (*n*=6). (**g**) Computation of the Ripley K function [$K(r)$, with r being the distance in pixels from one cell to the closest one] to determine the distribution pattern of PDX1$^+$KI67$^+$ progenitors in 2D images at PCW7, 9 and 11. Red lines represent the random distribution while each black line represents the quantification of $K(r)$ for PDX1$^+$KI67$^+$ progenitors in a single 2D image. (**h**) Expected output of $K(r)$ computed for three different types of spatial distribution: random, aggregate and regular. (**i**) Determination of the cell identity of peripheral pancreatic cells. CPA1 in green and KI67 in red in a human fetal pancreas at PCW11. Scale bars: 100 μm (**a**, **c**), 500 μm (**f**), 1 mm (**i**)

The next question concerned the spatial location of proliferating progenitors. We took advantage from recurrent access to fresh pancreases and used EdU, a thymidine analogue, to label cells entering S-phase. Proliferating pancreatic progenitors (PDX1$^+$EdU$^+$) were found to be highly enriched at the periphery of the pancreas, while their frequency in the centre was extremely low (Fig. 3f). The distribution pattern of pancreatic proliferating progenitors was mathematically analysed by computing the Ripley K function [$K(r)$] [18] in 2D images at PCW7, 9 and 11. It showed that PDX1$^+$KI67$^+$ progenitors are clustered together in aggregates, rather than randomly distributed (Fig. 3g,h). We finally determined whether proliferating PDX1$^+$KI67$^+$ cells might represent acinar cells that express CPA1. We observed that the human fetal pancreas is enriched in CPA1$^+$ cells in the periphery, rather than in the centre (Fig. 3i), further supporting that the inner fetal pancreas is an endocrine niche. We also found that the majority of these CPA1$^+$ cells lacked KI67 expression. Hence, the fact that most of the proliferating peripheral cells are not CPA1$^+$ sustains the idea that these cells are progenitors rather than differentiated acinar cells. Overall, our data further support the existence of a niche of proliferation for pancreatic progenitors in the periphery of the human embryonic and fetal pancreas.

PDGFAA induces the proliferation of human pancreatic progenitors in vitro We finally searched for signalling pathways that induce the proliferation of human pancreatic progenitors. For this purpose, we cultured human fetal pancreases over a floating filter disk in a gas–liquid interface for either 3 or 7 days. Under such conditions, pancreatic progenitors were maintained up to 7 days keeping a similar proliferation ratio (16.94±7.72% and 14.54±0.78% of PDX1$^+$ cells at day 3 and 7, respectively, mean ± SD, *n*=5–6 per group) than in vivo (19.98±2.42%, mean ± SD, *n*=3 at PCW9) (ESM Fig. 4a). Furthermore, the progenitors kept their multipotent phenotype during the full culture period, as assessed by the expression of PDX1 and NKX6.1 (ESM Fig. 4b). Gain- and loss-of-function experiments using either fibroblast growth factor (FGF)10 [28] or the mitogen-activated protein kinase kinase 1 (MEK1) inhibitor PD98059 [29], respectively, did not alter the PDX1$^+$KI67$^+$ ratio (data not shown). We next switched to a culture medium that contains ALK5i, noggin and nicotinamide that showed a reduction in the PDX1$^+$/KI67$^+$ ratio to around 5% to be used to search for factors that enhance progenitor proliferation. Our previous transcriptomic data [14] indicated that PDGF receptor α (PDGFRA) and PDGF receptor β (PDGFRB) are specifically expressed by human fetal pancreatic mesenchyme but not in pancreatic epithelial cells (Fig. 4a) and we further confirmed such data by immunostaining (Fig. 4b,c). We thus treated pancreatic explants with PDGFAA for 7 days. The macroscopic architecture of the explants remained unaffected (Fig. 4d). We observed a threefold increase in the number of proliferating progenitors (PDX1$^+$KI67$^+$) (Fig. 4e). We also observed changes in the microscopic tissue architecture following PDGFAA treatment. While the lumen size increased in control explants during the culture period, upon PDGFAA treatment, their size became more similar to that observed in vivo (Fig. 4f,g). Overall, through the establishment of a culture model of human fetal pancreases, we suggested that PDGF acts indirectly through mesenchymal cells to induce progenitor cell proliferation.

Discussion

There is an urgent need to improve the development of stem cell-derived human beta cells, to build novel therapies for the treatment of type 1 diabetes [30]. Most of the current protocols attempt to recapitulate beta cell neogenesis processes [31, 32]. However, the vast majority of our knowledge on beta cell differentiation comes from studies on mouse pancreas development [3, 33] and a detailed timeline and topographic description of human embryonic and fetal pancreatic cell proliferation and differentiation remained to be established. Here, through the Inserm-funded HuDeCA consortium (https://hudeca.genouest.org/), we could access a large collection of fresh pancreases between PCW5 and PCW11.

The majority of previous histological data on the developing mouse and human pancreas has been generated using conventional 2D sections [7, 8, 34]. Recently, a 3D
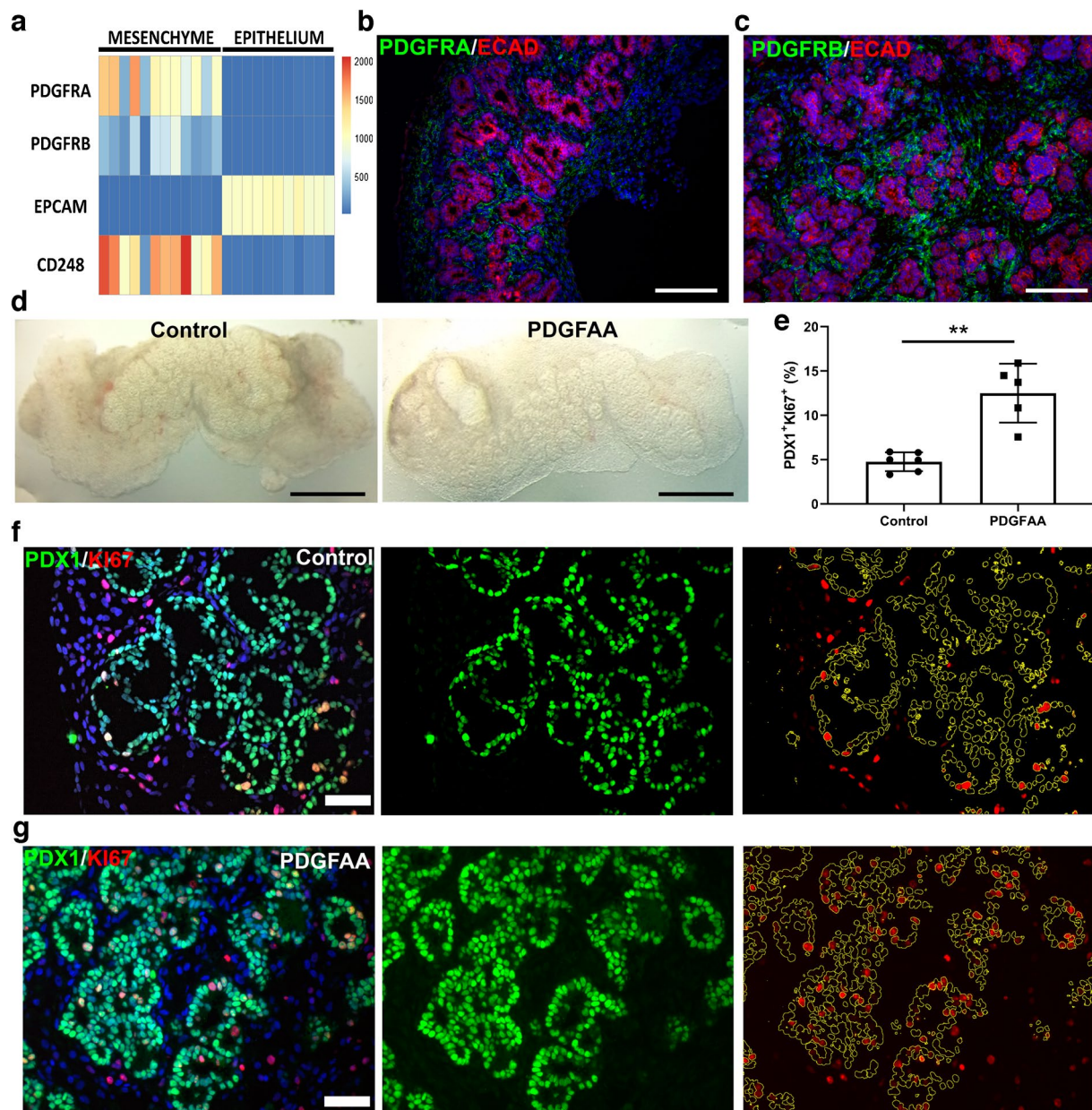
Fig. 4 Effect of PDGFAA in explants of human embryonic and fetal pancreases. (**a**) Heatmap showing the expression of PDGFRA and PDGFRB in the mesenchymal and epithelial fraction of human fetal pancreases. Epithelial (epithelial cellular adhesion molecule [EPCAM]) and mesenchymal (CD248) markers are used as positive controls for each population. The heatmap was generated as described in the legend for Fig. 3e with expression values from Ramond et al 2017 [14]. (**b**, **c**) Expression pattern of PDGFRA and PDGFRB (green) in a human fetal pancreas at PCW10, ECAD is in red. (**d**) Macroscopic integrity of the tissue at day 7 of culture in control or treated samples. (**e**) Determination of the proliferation ratio for pancreatic progenitors at day 7 cultured in DMEM/F12 supplemented medium treated or not with PDFGAA (n=5–6). Mean ± SD. (**f**, **g**) Representative images of control and treated (PDGFAA) samples at day 7 cultured in DMEM/F12 supplemented medium stained with PDX1 (green) and KI67 (red). Scale bars: 150 μm (**b**, **c**, **f**, **g**), 1 mm (**d**)

description of the developing mouse pancreas was published [35]. It provided a comprehensive view of the cellular composition and topological relationships of embryonic pancreatic cells. Here, we employed a similar pipeline to generate the first 3D atlas of the developing human pancreas by in toto staining, tissue clearing and LSFM imaging. We focused on the first trimester, when first endocrine cells are generated [7]. An interesting observation is our detection of two pancreatic buds, ventral and dorsal, prior to their fusion. We also detected the first INS+ cells in the dorsal pancreas, similar to what has been described in mouse and zebrafish embryonic pancreases [24, 36]. Here we could

detect INS^{+} cells at around PCW5, 2 weeks earlier than previously described [8]. We also confirm the existence of extra-pancreatic INS^{+} cells in the gut region adjacent to the pancreas [25].

Our data show that the earliest INS^{+} cells are either isolated or form very small clusters (of about 4–5 cells), when in adults, islets contain hundreds of INS^{+} cells. Using KI67, we found that human embryonic and fetal INS^{+} cells exhibit a low proliferation rate. This suggests that islets do not form by proliferation in situ of preexisting INS^{+} cells, consistent with our previous data [37]. Additionally, similar observations from mouse chimeras further support the polyclonal origin of pancreatic islets [38, 39]. We thus postulate that in humans, mature islets form by the aggregation of preexisting INS^{+} cells. Mouse data suggest that endocrine cell differentiation is followed by epithelial–mesenchymal transition, migration and aggregation [40]. However, in an alternative hypothesis, INS^{+} cells could differentiate from endocrine progenitors located within a single epithelial cord while maintaining contact with this structure, forming a peninsula and then an islet [41].

We raised questions regarding the earliest INS^{+} cells and their location. INS^{+} cells were preferentially located in the centre of the pancreas where they were tightly aligned, while almost absent in the periphery, suggesting the existence of a highly specific differentiation niche for endocrinogenesis in the inner part of the pancreas. We can speculate that endocrine progenitors expressing the transcription factor neurogenin3 (NGN3) are also located in the centre of the developing human pancreas. However, we could not validate experimentally that point as we were unable to find a suitable NGN3 antibody compatible with our 3D staining approach. Signals controlling this specific spatial pattern of differentiation remain unknown. Although vascularisation has been shown to play major roles in mouse beta cell development [26, 42, 43], we did not observe a correlation between the location of INS^{+} cells and the vascular tree. Whether the specific location of the first human INS^{+} cells is influenced by nerves, an important player in beta cell physiology [44], remains to be explored. We are also testing the hypothesis that the mesenchyme located in the inner and peripheral regions of the pancreas are different.

Our KI67 data indicate that the proliferation rate of INS^{+} cells is extremely limited during the second part of the first trimester of gestation, about 20 times lower than pancreatic progenitors. This demonstrates that the amplification pool for endocrinogenesis is at the level of pancreatic progenitors and not INS^{+} cells. This is in agreement with data obtained in mouse embryos where fetal pancreatic progenitors proliferate far more efficiently than beta cells and their number is increased by growth factors such as FGF7 and FGF10 [22, 29]. We observed that, in contrast with INS^{+} cells, progenitor proliferation is restricted to the periphery of the pancreas.

These findings suggest that endocrine cell differentiation and progenitor proliferation are differentially regulated processes during human pancreatic development.

Here, we developed a culture system to study human progenitor cell proliferation, using a strategy previously used in rat embryos [22]. Accordingly, we found that in human embryonic pancreas cultures progenitors proliferate for at least 7 days at a similar ratio to in vivo. By using this model, we demonstrate that PDGFAA, a molecule produced in the fetal pancreas by epithelial [45] and vascular smooth muscle [46] cells, enhances the proliferation of pancreatic progenitors. Recently, *PDGFRA* mRNA was found to be enriched in the pancreatic mesenchyme [45, 46], in agreement with our transcriptomic data [14] and with single cell transcriptomic data derived from the DESCARTES Atlas (https://descartes.brotmanbaty.org/, last accessed 7 February 2024). We confirmed here that the expression of PDGFRA and PDGFRB is restricted to the pancreatic mesenchyme, suggesting that PDGF exerts an indirect influence on progenitors by affecting mesenchymal cells.

Altogether, we present here the first attempt to build a 3D atlas of the developing human pancreas. Overall, this resource sheds light on the genesis and location of the first INS^{+} cells, as well as pancreatic proliferating progenitors. Furthermore, we also describe the mitogenic effect of PDGFAA in the pancreatic epithelium. Our 3D imaging pipeline will allow researchers to explore the developing anatomy of the pancreas in a spatial context, and to visualise the relationships between different structures and cell types. Thus, this 3D atlas should be further expanded by mapping other endocrine cells such as glucagon- and somatostatin-expressing cells. This information holds great potential for enhancing our understanding of the underlying mechanisms driving embryonic and fetal pancreatic development, and potentially this knowledge could further improve the generation of stem cell-derived beta cells.

References

1. Shih HP, Wang A, Sander M (2013) Pancreas organogenesis: from lineage determination to morphogenesis. Annu Rev Cell Dev Biol 29:81–105. https://doi.org/10.1146/ANNUREV-CELLBIO-101512-122405

2. Atkinson MA, Campbell-Thompson M, Kusmartseva I, Kaestner KH (2020) Organisation of the human pancreas in health and in diabetes. Diabetologia 63(10):1966–1973. https://doi.org/10.1007/s00125-020-05203-7

3. Pan FC, Wright C (2011) Pancreas organogenesis: from bud to plexus to gland. Dev Dyn 240(3):530–565. https://doi.org/10.1002/DVDY.22584

4. Siehler J, Blöchinger AK, Meier M, Lickert H (2021) Engineering islets from stem cells for advanced therapies of diabetes. Nat Rev Drug Discov 20(12):920–940. https://doi.org/10.1038/S41573-021-00262-W

5. Isaacson A, Spagnoli FM (2021) Pancreatic cell fate specification: insights into developmental mechanisms and their application for lineage reprogramming. Curr Opin Genet Dev 70:32–39. https://doi.org/10.1016/J.GDE.2021.05.003

6. Gittes GK (2009) Developmental biology of the pancreas: a comprehensive review. Dev Biol 326:4–35. https://doi.org/10.1016/j.ydbio.2008.10.024

7. Jennings RE, Berry AA, Strutt JP, Gerrard DT, Hanley NA (2015) Human pancreas development. Development 142:3126–3137. https://doi.org/10.1242/dev.120063

8. Jennings RE, Berry AA, Kirkwood-Wilson R et al (2013) Development of the human pancreas from foregut to endocrine commitment. Diabetes 62(10):3514–3522. https://doi.org/10.2337/DB12-1479

9. Jennings RE, Scharfmann R, Staels W (2020) Transcription factors that shape the mammalian pancreas. Diabetologia 63(10):1974–1980. https://doi.org/10.1007/S00125-020-05161-0

10. Renier N, Wu Z, Simon DJ, Yang J, Ariel P, Tessier-Lavigne M (2014) IDISCO: a simple, rapid method to immunolabel large tissue samples for volume imaging. Cell 159(4):896–910. https://doi.org/10.1016/j.cell.2014.10.010

11. Belle M, Godefroy D, Dominici C et al (2014) A simple method for 3D Analysis of immunolabeled axonal tracts in a transparent nervous system. Cell Rep 9(4):1191–1201. https://doi.org/10.1016/j.celrep.2014.10.037

12. Susaki EA, Tainaka K, Perrin D et al (2014) Whole-brain imaging with single-cell resolution using chemical cocktails and computational analysis. Cell 157(3):726–739. https://doi.org/10.1016/j.cell.2014.03.042

13. Belle M, Godefroy D, Couly G et al (2017) Tridimensional visualization and analysis of early human development. Cell 169(1):161-173.e12. https://doi.org/10.1016/j.cell.2017.03.008

14. Ramond C, Glaser N, Berthault C et al (2017) Reconstructing human pancreatic differentiation by mapping specific cell populations during development. Elife 6:e27564. https://doi.org/10.7554/ELIFE.27564

15. Ramond C, Beydag-Tasöz BS, Azad A et al (2018) Understanding human fetal pancreas development using subpopulation sorting, RNA sequencing and single-cell profiling. Development 145(16):dev165480. https://doi.org/10.1242/DEV.165480

16. Evtouchenko L, Studer L, Spencer C, Dreher E, Seiler RW (1996) A mathematical model for the estimation of human embryonic and fetal age. Cell Transplant 5(4):453–464. https://doi.org/10.1016/0963-6897(96)00079-6

17. Huijbregts L, Petersen MBK, Berthault C et al (2019) Bromodomain and extra terminal protein inhibitors promote pancreatic endocrine cell fate. Diabetes 68(4):761–773. https://doi.org/10.2337/db18-0224

18. Dixon PM (2012) Ripley's K function. Encycl Environmetrics. https://doi.org/10.1002/9780470057339.var046.pub2

19. Schindelin J, Arganda-Carreras I, Frise E et al (2012) Fiji: an open-source platform for biological-image analysis. Nat Methods 9(7):676–682. https://doi.org/10.1038/nmeth.2019

20. Baddeley A, Rubak E, Turner R (2015) Spatial point patterns: methodology and applications with R. Chapman & Hall, New York. https://doi.org/10.1201/B19708

21. Renier N, Adams EL, Kirst C et al (2016) Mapping of brain activity by automated volume analysis of immediate early genes. Cell 165(7):1789–1802. https://doi.org/10.1016/J.CELL.2016.05.007

22. Attali M, Stetsyuk V, Basmaciogullari A et al (2007) Control of beta-cell differentiation by the pancreatic mesenchyme. Diabetes 56(5):1248–1258. https://doi.org/10.2337/DB06-1307

23. Slack JMW (1995) Developmental biology of the pancreas. Development 121(6):1569–1580. https://doi.org/10.1242/DEV.121.6.1569

24. Herrera PL, Huarte J, Sanvito F, Meda P, Orci L, Vassalli JD (1991) Embryogenesis of the murine endocrine pancreas; early expression of pancreatic polypeptide gene. Development 113(4):1257–1265. https://doi.org/10.1242/DEV.113.4.1257

25. Egozi A, Llivichuzhca-Loja D, McCourt BT et al (2021) Insulin is expressed by enteroendocrine cells during human fetal development. Nat Med 27(12):2104–2107. https://doi.org/10.1038/S41591-021-01586-1

26. Lammert E, Cleaver O, Melton D (2001) Induction of pancreatic differentiation by signals from blood vessels. Science 294(5542):564–567. https://doi.org/10.1126/SCIENCE.1064344

27. Scharfmann R, Pechberty S, Hazhouz Y et al (2014) Development of a conditionally immortalized human pancreatic β cell line. J Clin Invest 124(5):2087–2098. https://doi.org/10.1172/JCI72674

28. Miralles F, Czernichow P, Ozaki K, Itoh N, Scharfmann R (1999) Signaling through fibroblast growth factor receptor 2b plays a key role in the development of the exocrine pancreas. Proc Natl Acad Sci U S A 96(11):6267–6272. https://doi.org/10.1073/pnas.96.11.6267

29. Elghazi L, Cras-Méneur C, Czernichow P, Scharfmann R (2002) Role for FGFR2IIIb-mediated signals in controlling pancreatic endocrine progenitor cell proliferation. Proc Natl Acad Sci U S A 99(6):3884–3889. https://doi.org/10.1073/pnas.062321799

30. Balboa D, Iworima DG, Kieffer TJ (2021) Human pluripotent stem cells to model islet defects in diabetes. Front Endocrinol (Lausanne) 12:642152. https://doi.org/10.3389/FENDO.2021.642152

31. Pagliuca FW, Millman JR, Gürtler M et al (2014) Generation of functional human pancreatic β cells in vitro. Cell 159(2):428–439. https://doi.org/10.1016/J.CELL.2014.09.040

32. Hogrebe NJ, Maxwell KG, Augsornworawat P, Millman JR (2021) Generation of insulin-producing pancreatic β cells from multiple human stem cell lines. Nat Protoc 16(9):4109–4143. https://doi.org/10.1038/S41596-021-00560-Y

33. Sever D, Grapin-Botton A (2020) Regeneration of the pancreas: proliferation and cellular conversion of surviving cells. Curr Opin Genet Dev 64:84–93. https://doi.org/10.1016/J.GDE.2020.06.005

34. Henry BM, Skinningsrud B, Saganiak K, Pękala PA, Walocha JA, Tomaszewski KA (2019) Development of the human pancreas and its vasculature — an integrated review covering anatomical, embryological, histological, and molecular aspects. Ann Anat 221:115–124. https://doi.org/10.1016/j.aanat.2018.09.008

35. Glorieux L, Sapala A, Willnow D et al (2022) Development of a 3D atlas of the embryonic pancreas for topological and quantitative analysis of heterologous cell interactions. Development 149(3):dev199655. https://doi.org/10.1242/DEV.199655

36. Hesselson D, Anderson RM, Beinat M, Stainier DYR (2009) Distinct populations of quiescent and proliferative pancreatic β-cells identified by HOTcre mediated labeling. Proc Natl Acad Sci U S A 106(35):14896–14901. https://doi.org/10.1073/PNAS.0906348106/SUPPL_FILE/0906348106SI.PDF

37. Scharfmann R, Xiao X, Heimberg H, Mallet J, Ravassard P (2008) Beta cells within single human islets originate from multiple progenitors. PLoS One 3(10):e3559. https://doi.org/10.1371/JOURNAL.PONE.0003559

38. Deltour L, Leduque P, Paldi A, Ripoche MA, Dubois P, Jami J (1991) Polyclonal origin of pancreatic islets in aggregation mouse chimaeras. Development 112(4):1115–1121. https://doi.org/10.1242/DEV.112.4.1115

39. Scott Swenson E, Xanthopoulos J, Nottoli T, McGrath J, Theise ND, Krause DS (2009) Chimeric mice reveal clonal development of pancreatic acini, but not islets. Biochem Biophys Res Commun 379(2):526–531. https://doi.org/10.1016/J.BBRC.2008.12.104

40. Gouzi M, Kim YH, Katsumoto K, Johansson K, Grapin-Botton A (2011) Neurogenin3 initiates stepwise delamination of differentiating endocrine cells during pancreas development. Dev Dyn 240(3):589–604. https://doi.org/10.1002/DVDY.22544

41. Sharon N, Chawla R, Mueller J et al (2019) A peninsular structure coordinates asynchronous differentiation with morphogenesis to generate pancreatic islets. Cell 176(4):790-804.e13. https://doi.org/10.1016/J.CELL.2018.12.003

42. Edsbagge J, Johansson JK, Esni F, Luo Y, Radice GL, Semb H (2005) Vascular function and sphingosine-1-phosphate regulate development of the dorsal pancreatic mesenchyme. Development 132(5):1085–1092. https://doi.org/10.1242/DEV.01643

43. Jacquemin P, Yoshitomi H, Kashima Y, Rousseau GG, Lemaigre FP, Zaret KS (2006) An endothelial-mesenchymal relay pathway regulates early phases of pancreas development. Dev Biol 290(1):189–199. https://doi.org/10.1016/J.YDBIO.2005.11.023

44. Ahrén B (2000) Autonomic regulation of islet hormone secretion–implications for health and disease. Diabetologia 43(4):393–410. https://doi.org/10.1007/S001250051322

45. Gonçalves CA, Larsen M, Jung S et al (2021) A 3D system to model human pancreas development and its reference single-cell transcriptome atlas identify signaling pathways required for progenitor expansion. Nat Commun 12(1):3144. https://doi.org/10.1038/S41467-021-23295-6

46. Sean de la O, Liu Z, Sun H et al (2022) Single-cell multi-omic roadmap of human fetal pancreatic development. BioRxiv 480942 (Preprint). 18 Feb 2022. Available from: https://doi.org/10.1101/2022.02.17.480942

47. Duvillié B, Attali M, Aiello V, Quemeneur E, Scharfmann R (2003) Label-retaining cells in the rat pancreas: location and differentiation potential in vitro. Diabetes 52(8):2035–2042. https://doi.org/10.2337/diabetes.52.8.2035